

Electronic Supporting Information (ESI) for Dalton Transactions

2018

Influence of the substituent on the phosphine ligand in novel rhenium (I) aldehydes. Synthesis, computational studies and first insights into antiproliferative activity

Michelle Muñoz-Osses^a, Daniel Siegmund^d, Alejandra Gómez^a, Fernando Godoy^{a, *}, Angélica Fierro^c, Leonel Llanos^b, Daniel Aravena^b and Nils Metzler-Nolte^{d, *}

^a Laboratory of Organometallic Chemistry, Faculty of Chemistry and Biology, Universidad de Santiago de Chile, Avenida Libertador Bernardo O'Higgins 3363. Estación Central. Santiago. Chile. E-mail: michelle.munoz@usach.cl ; fernando.godoy@usach.cl; alejandra.gomez@usach.cl

^b Laboratory of Computational Inorganic Chemistry, Faculty of Chemistry and Biology, Universidad de Santiago de Chile, Avenida Libertador Bernardo O'Higgins 3363. Estación Central. Santiago. Chile. E-mail: leonel.llanos@usach.cl ; daniel.aravena.p@usach.cl

^c Laboratory of Molecular Simulation, Department of Organic Chemistry, Faculty of Chemistry, Pontificia Universidad Católica de Chile, Avda. Vicuña Mackenna 4860, Macul, Santiago, Chile. E-mail: afierroh@uc.cl

^d Inorganic Chemistry I – Bioinorganic Chemistry, Faculty of Chemistry and Biochemistry, Ruhr University Bochum, Universitätsstrasse 150, 44797 Bochum, Germany. E-mail: nils.metzler-nolte@rub.de; daniel.Siegmund@ruhr-uni-bochum.de

Index

Experimental Section:

1. Synthesis and characterization of novel rhenium (I) dicarbonyl phosphine aldehydes.
 - a) NMR Spectrum of **2a-2c** compounds.
 - b) Electrochemical studies
 - c) Computational studies of rhenium (I) derivatives.
2. Cytotoxic studies of the new compounds in two cancer cell lines: HT-29 and PT-45.

1. Novel Rhenium dicarbonyl phosphine aldehydes $[(\eta^5\text{-C}_5\text{H}_4\text{CHO})\text{Re}(\text{CO})_2\text{PR}_3]$.

a) NMR Spectra

a.1. Synthesis of $[(\eta^5\text{-C}_5\text{H}_4\text{CHO})\text{Re}(\text{CO})_2\text{PMe}_3]$ (**2a**)

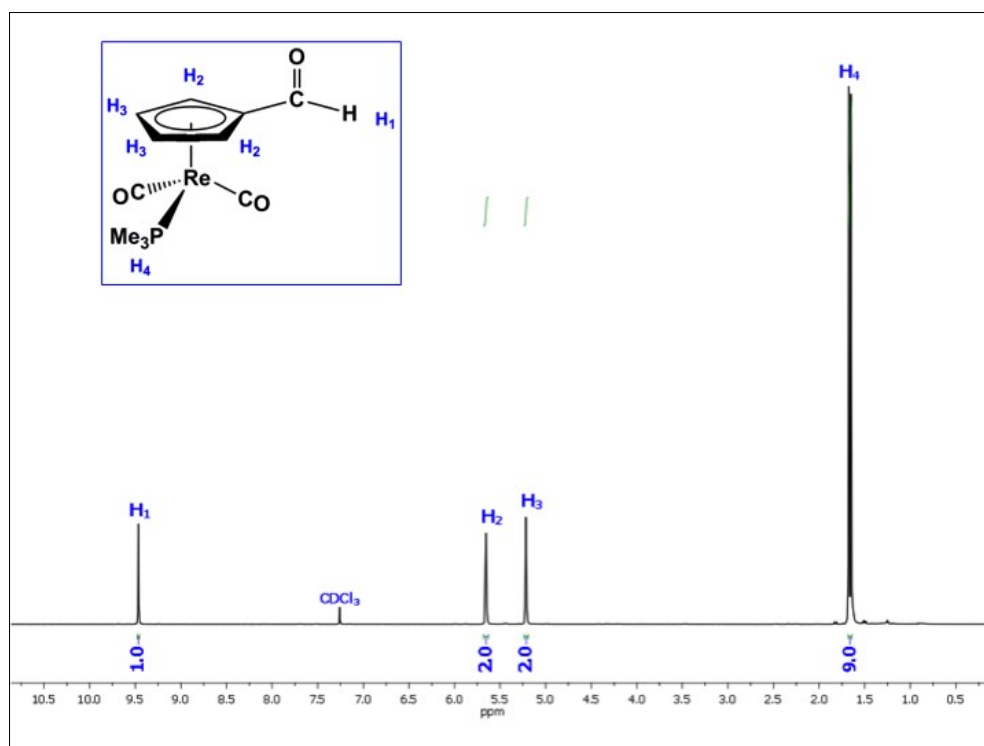


Figure S1. ^1H -NMR spectra (400 MHz) of a solution of **2a** (40 mM) in CDCl_3 at 298 K.

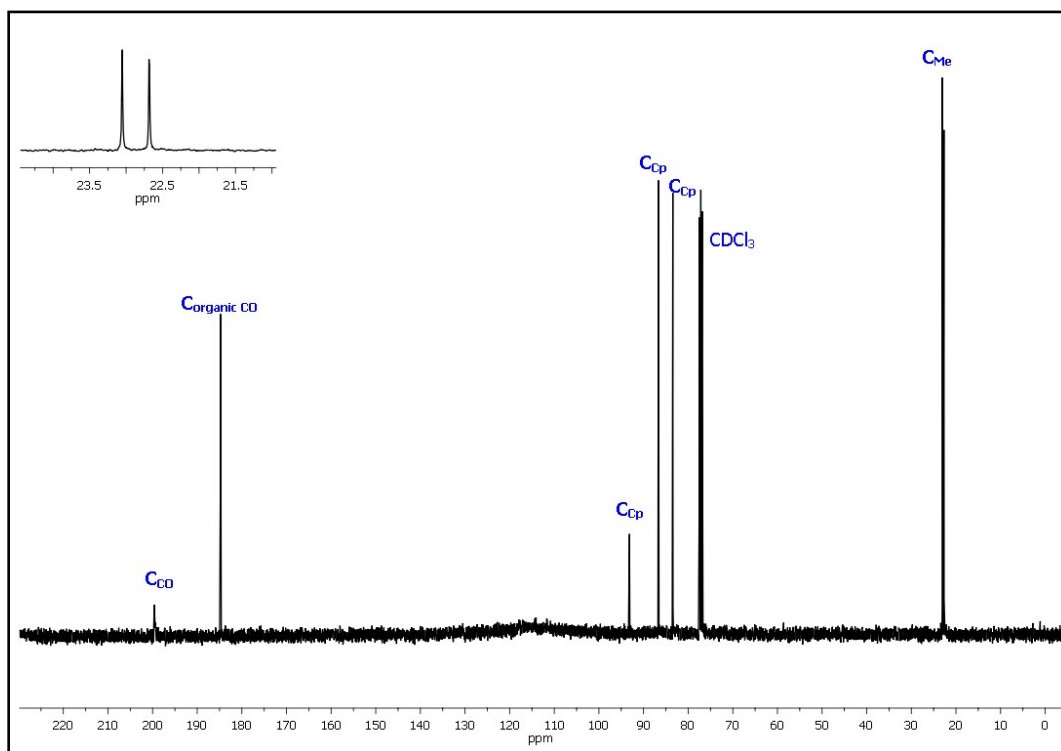


Figure S2. ^{13}C -NMR spectra (400 MHz) of a solution of **2a** (80 mM) in CDCl_3 at 298 K.

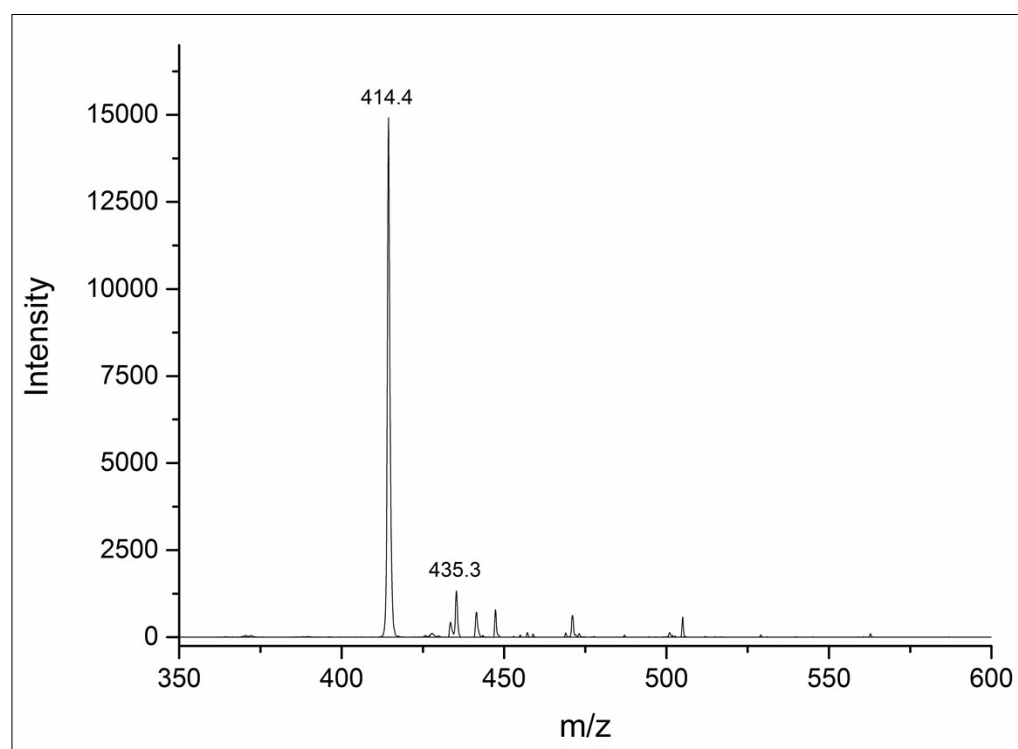


Figure S3. ESI-MS in CH_3CN of **2a** (1 mg/ml).

a.2. Synthesis of $[(\eta^5\text{-C}_5\text{H}_4\text{CHO})\text{Re}(\text{CO})_2\text{PPh}_3]$ (**2b**)

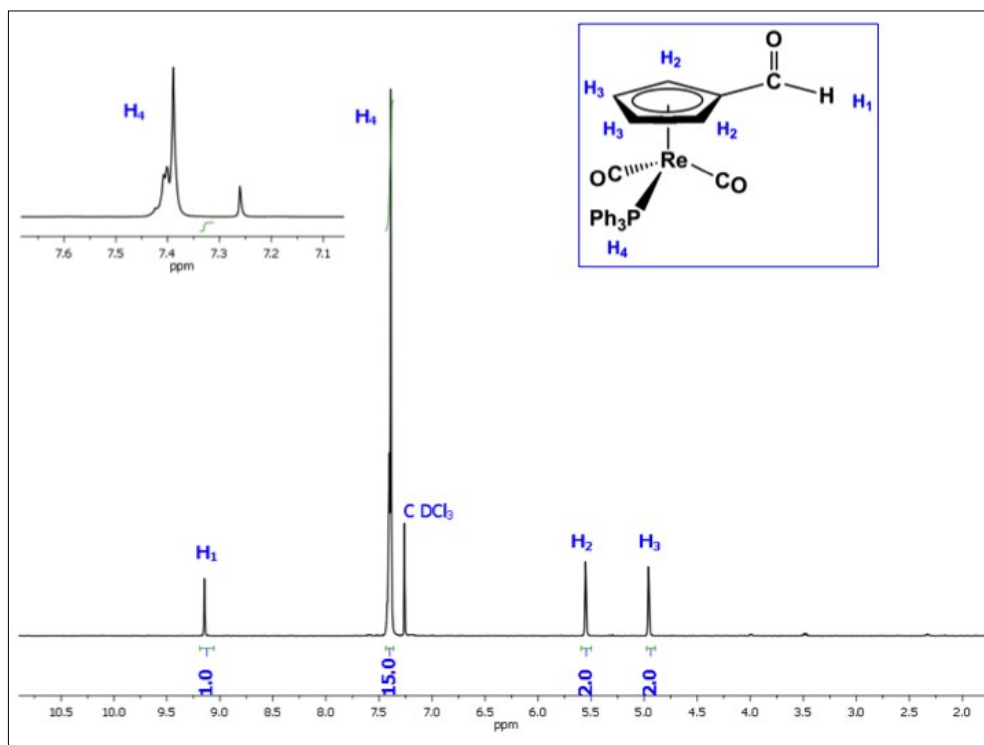


Figure S4. ^1H -NMR spectra (400 MHz) of a solution of **2b** (40 mM) in CDCl_3 at 298 K.

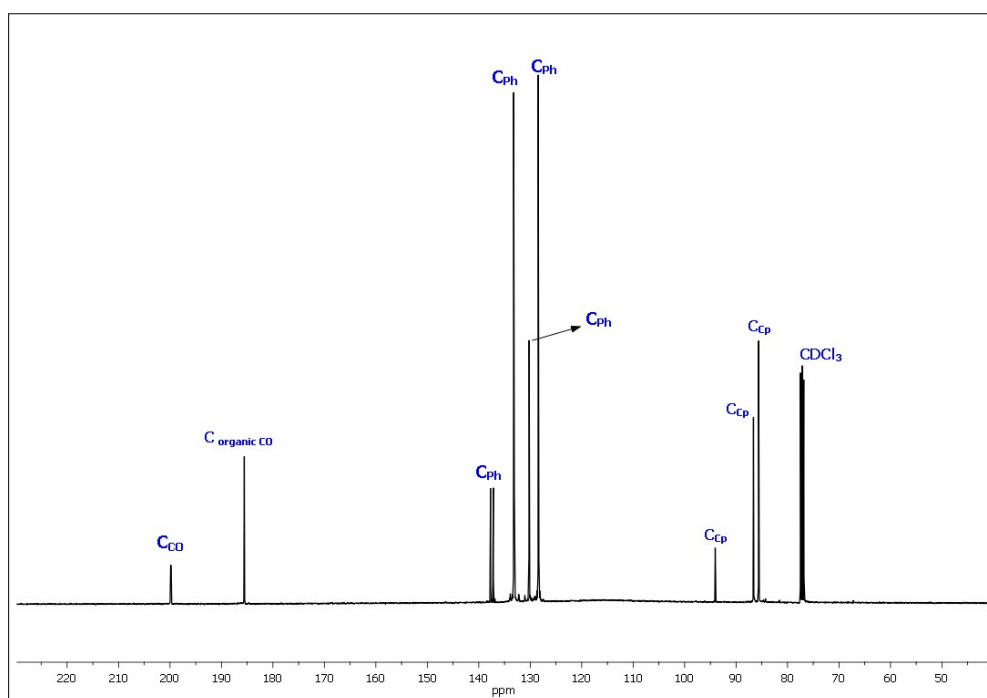


Figure S5. ^{13}C -NMR spectra (400 MHz) of a solution of **2b** (80 mM) in CDCl_3 at 298 K.

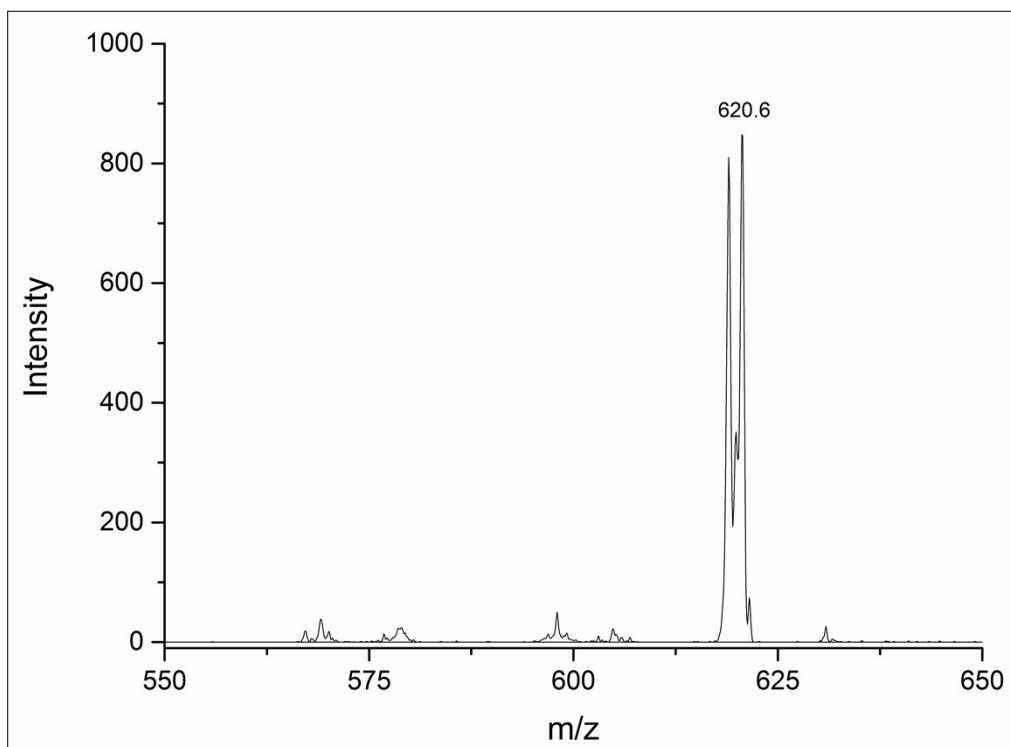


Figure S6. ESI-MS in CH₃CN of **2b** (1mg/ml).

a.3. Synthesis of $[(\eta^5\text{-C}_5\text{H}_4\text{CHO})\text{Re}(\text{CO})_2\text{PCy}_3]$ (2c**)**

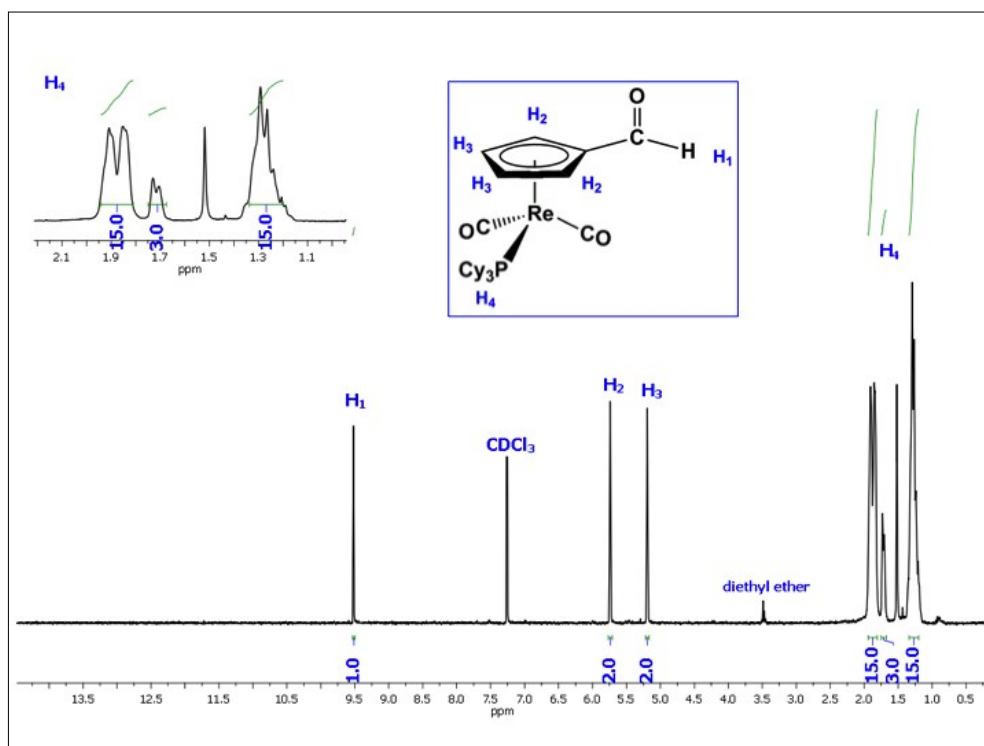


Figure S7. ¹H-NMR spectra (400 MHz) of a solution of **2c** (40 mM) in CDCl₃ at 298 K.

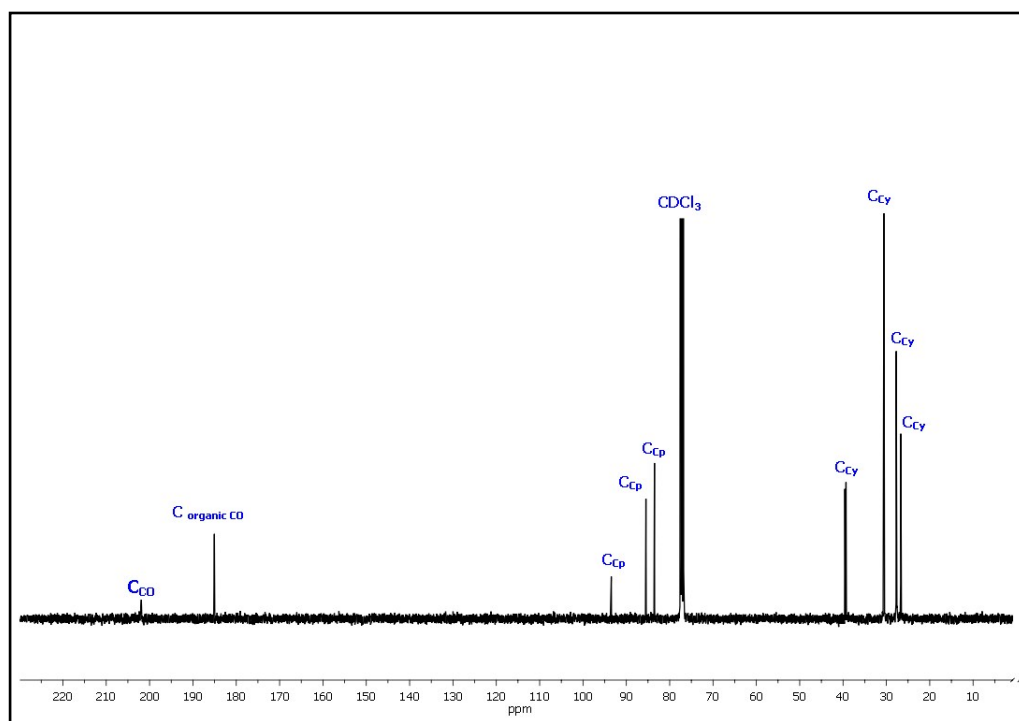


Figure S8. ^{13}C -NMR spectra (400 MHz) of a solution of **2c** (80 mM) in CDCl_3 at 298 K.

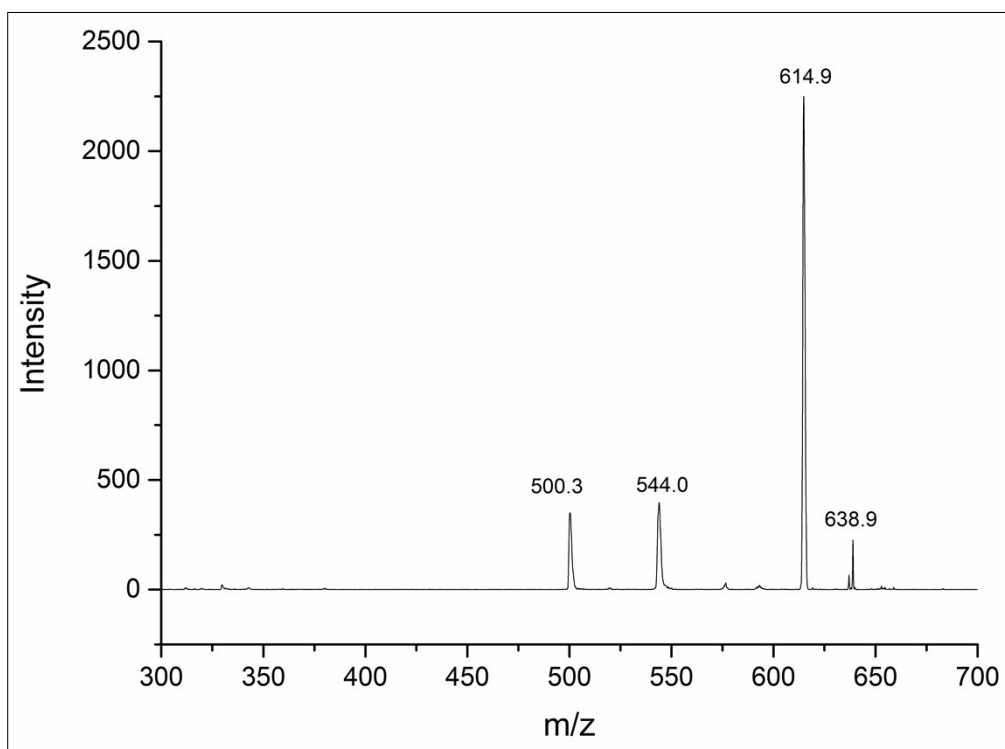


Figure S9. ESI-MS in CH_3CN of **2c** (1 mg/ml).

b) Electrochemical studies

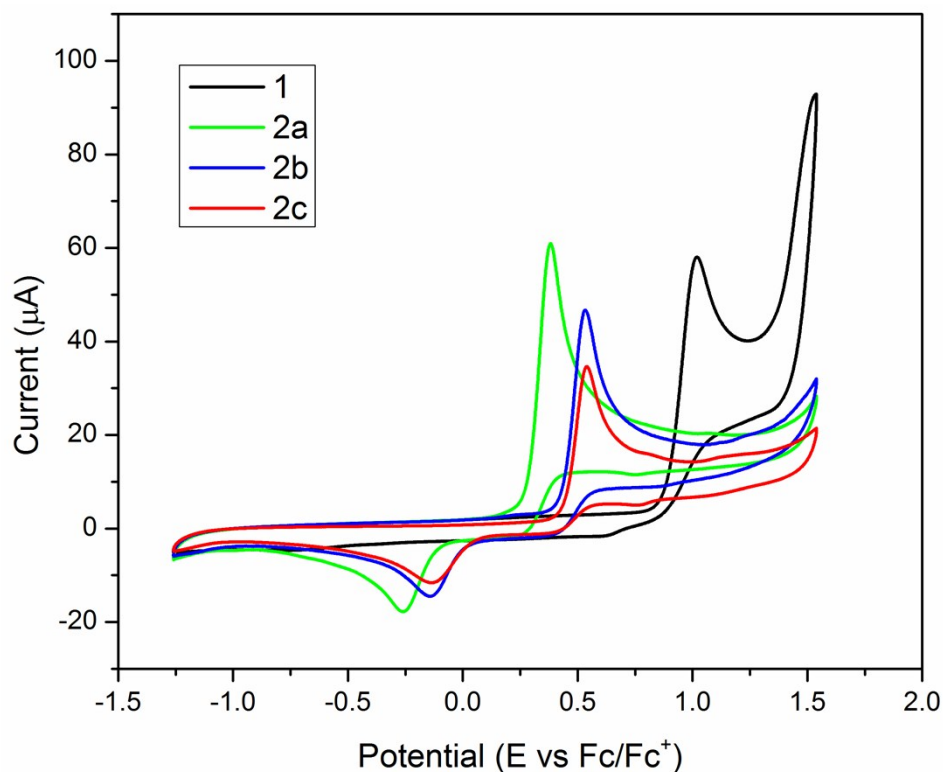


Figure S10. Cyclic voltammetry of phosphine derivatives **1** and **2a-c** (1mM), in dry CH₃CN using Bu₄NPF₆ (0.1 M) as the supporting electrolyte, at a scan rate of 100 mV/s.

c) Computational studies

Table S1: Experimental and calculated (DFT) frequencies ν_{CO} (cm⁻¹) of the symmetric and asymmetric stretching of the organometallic carbonyl ligand of each complex.

Compounds	Experimental	Calculated
1	2033, 1940	2048, 1944
2a	1935, 1867	1944, 1854
2b	1942, 1876	1957, 1872
2c	1928, 1860	1939, 1852

Table S2: Re-P distances from the DFT optimized structures

Compounds	Re-P (Å)
2a	2.36409
2b	2.36168
2c	2.40032

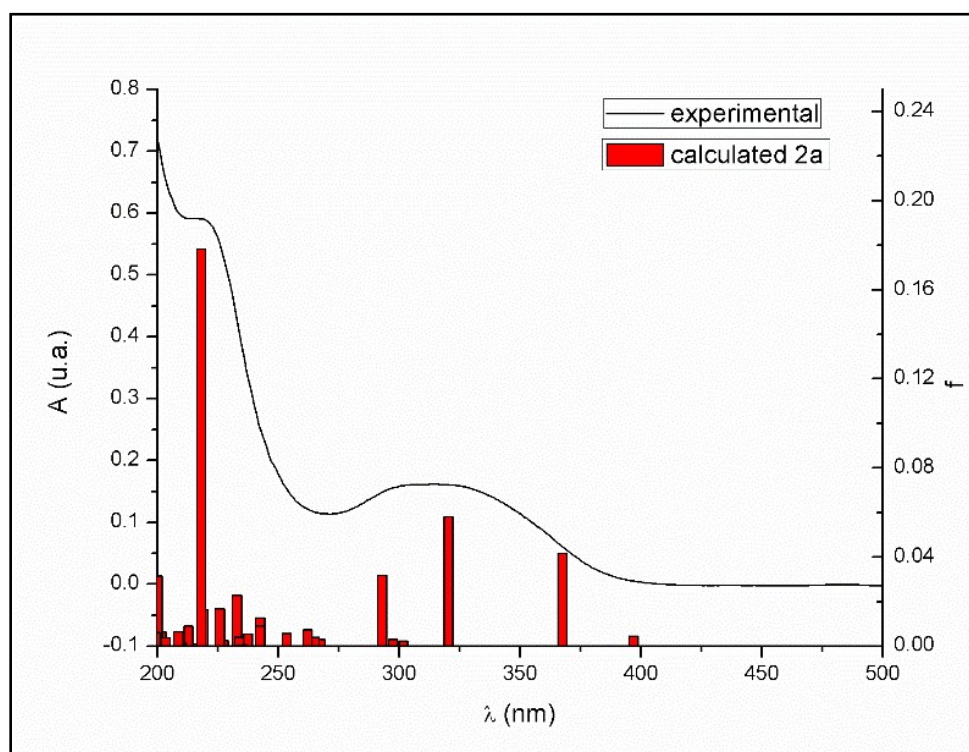


Figure S11. Experimental UV-Vis spectrum (black line) and electronic transitions (red bars) obtained for TD-DFT calculations of the complex **2a**.

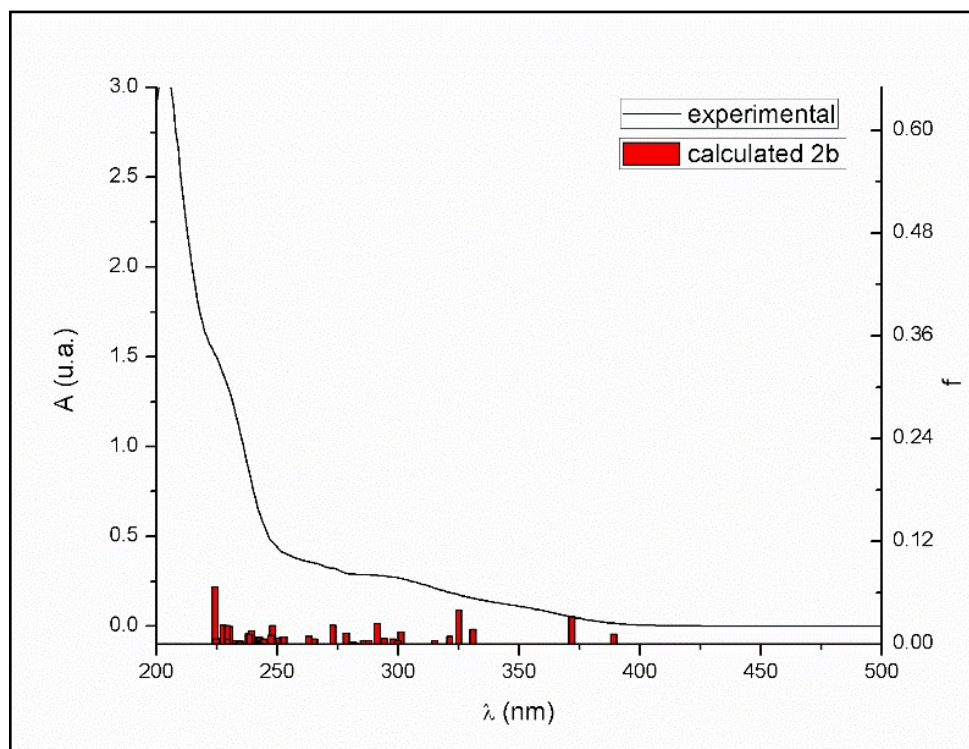


Figure S12. Experimental UV-Vis spectrum (black line) and electronic transitions (red bars) obtained for TD-DFT calculations of the complex **2b**.

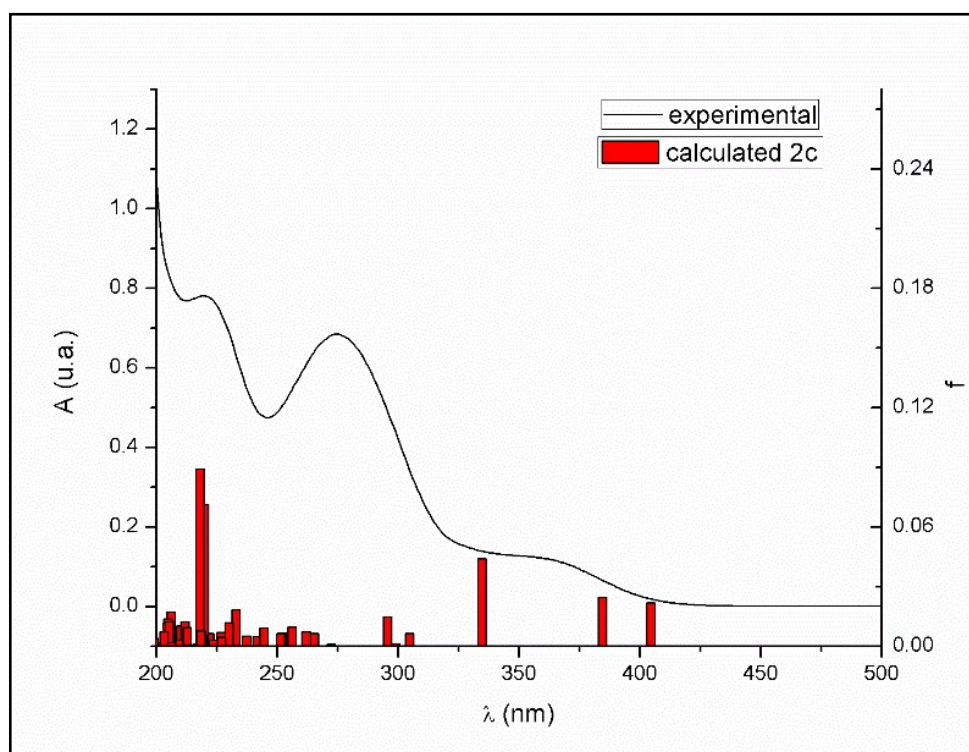


Figure S13. Experimental UV-Vis spectrum (black line) and electronic transitions (red bars) obtained for TD-DFT calculations of the complex **2c**.

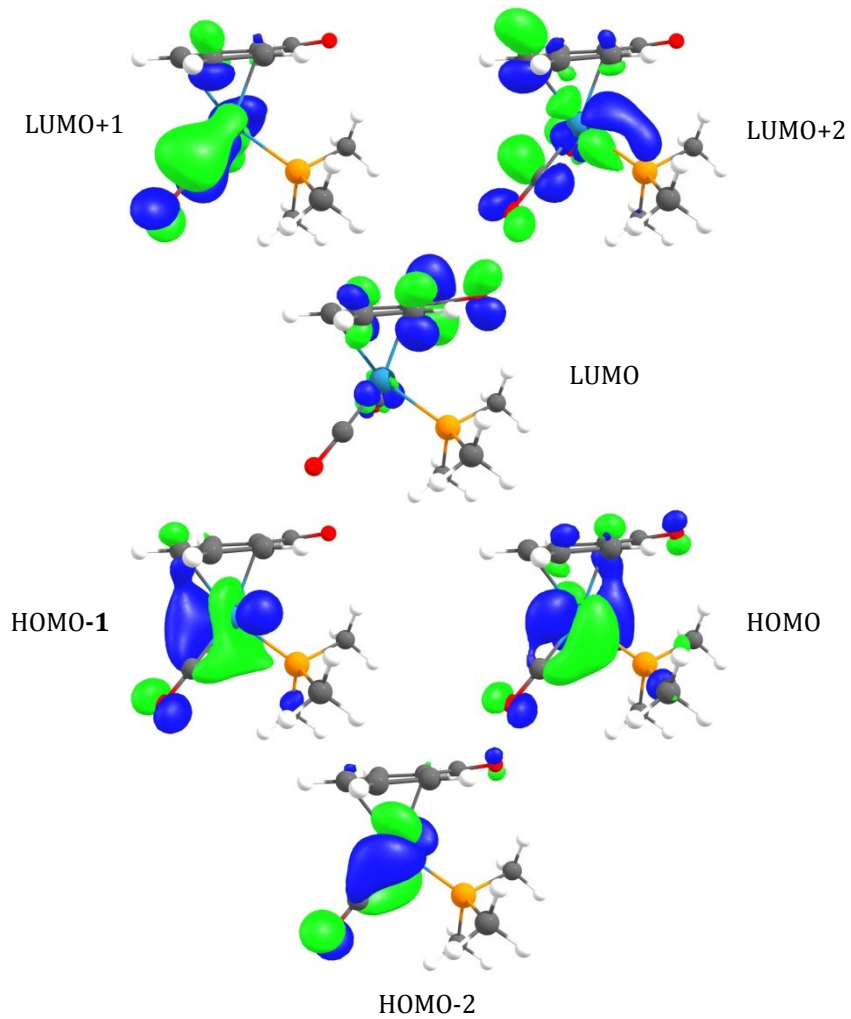


Figure S14. Calculated frontier orbitals of the complex **2a**.

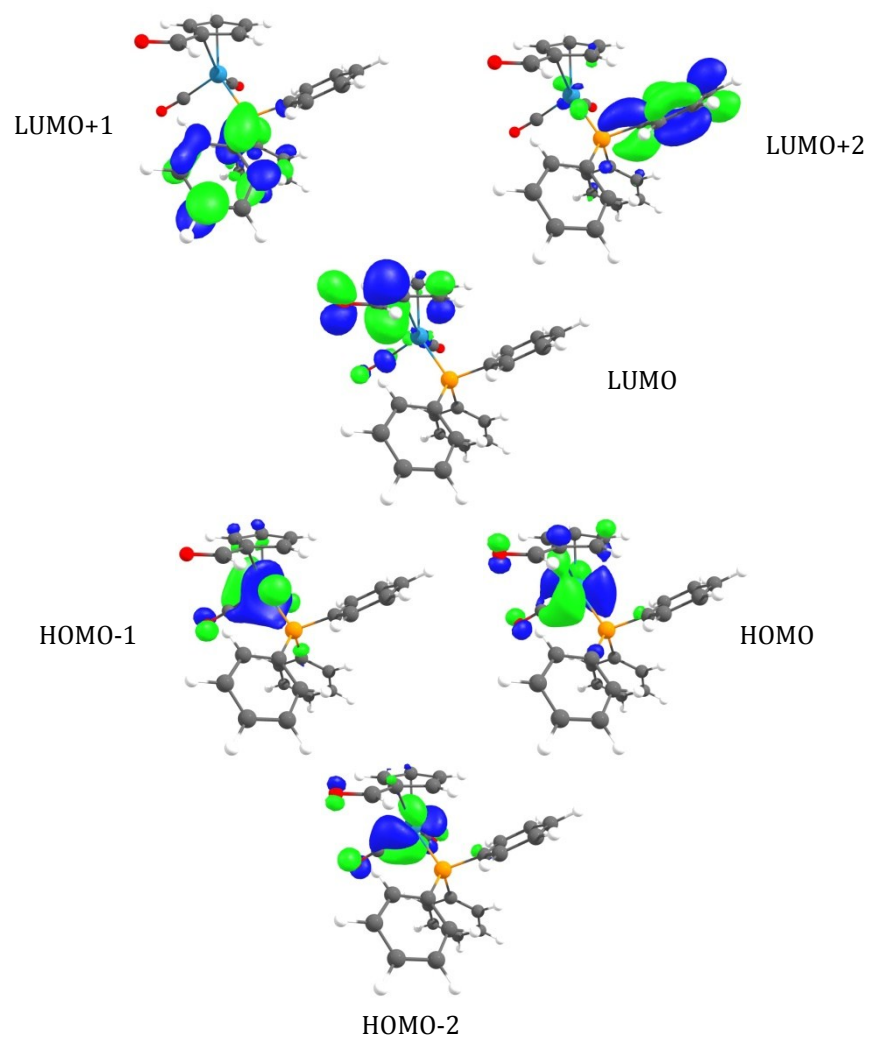


Figure S15. Calculated frontier orbitals of the complex **2b**.

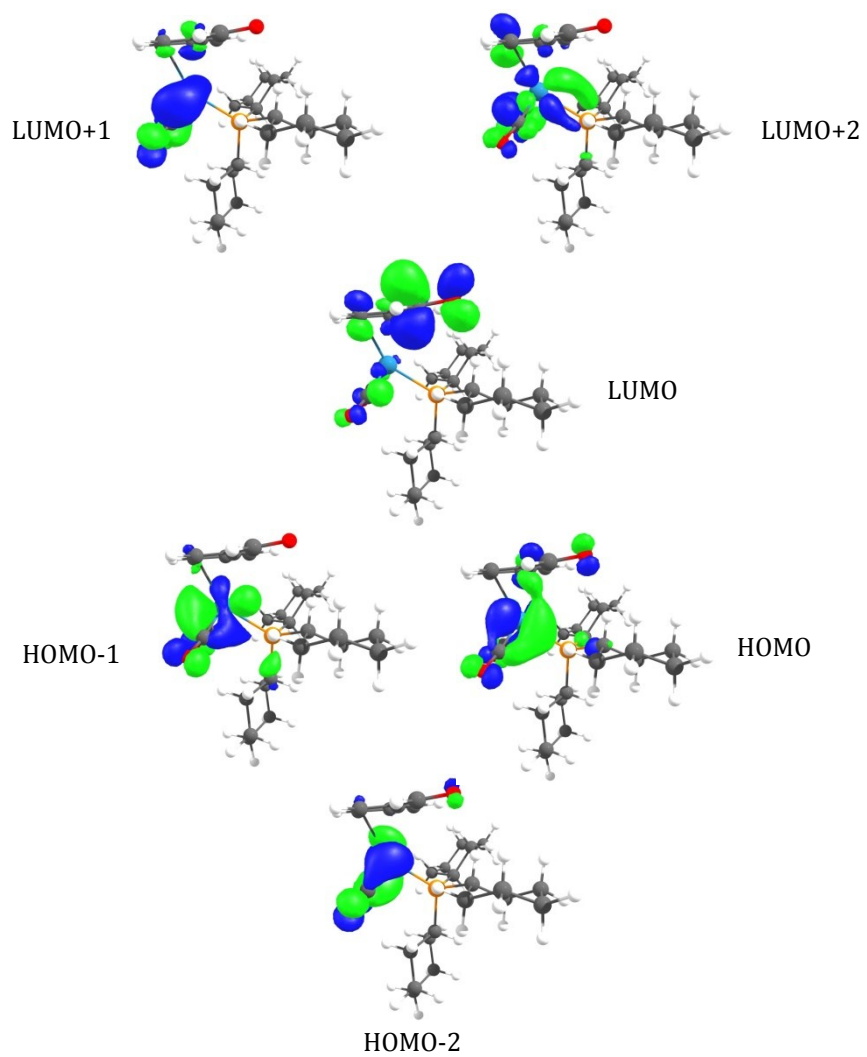


Figure S16. Calculated frontier orbitals of the complex **2c**.

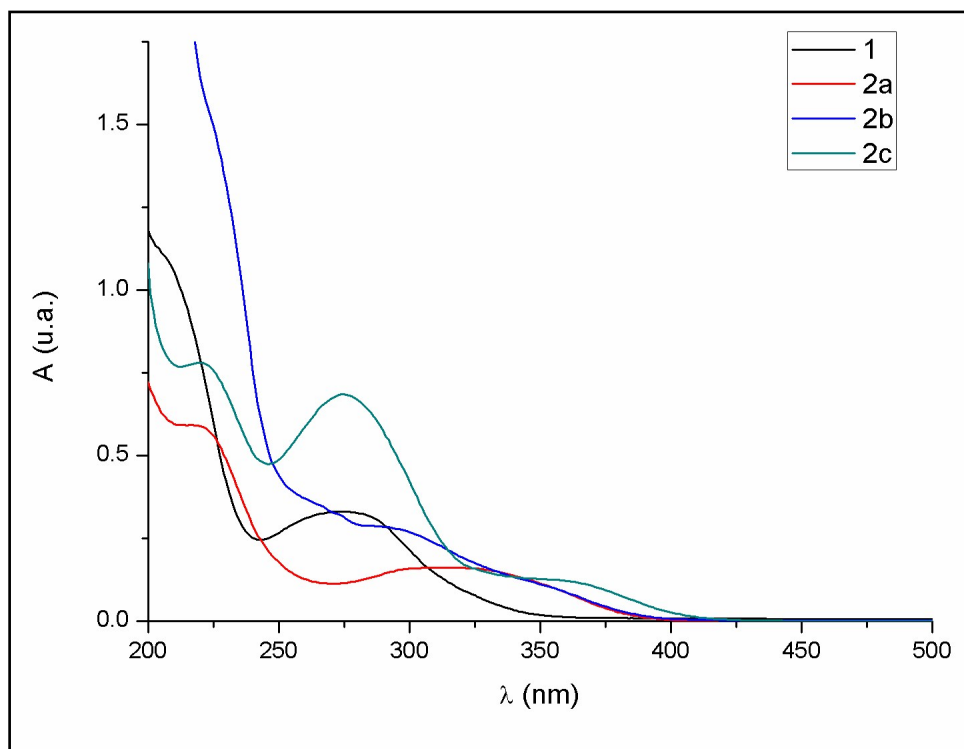


Figure S17. Experimental UV-Vis of 10^{-4} M solutions of **1**, **2a-c** complexes in CH_3CN at 298 K.

2. Cytotoxicity studies

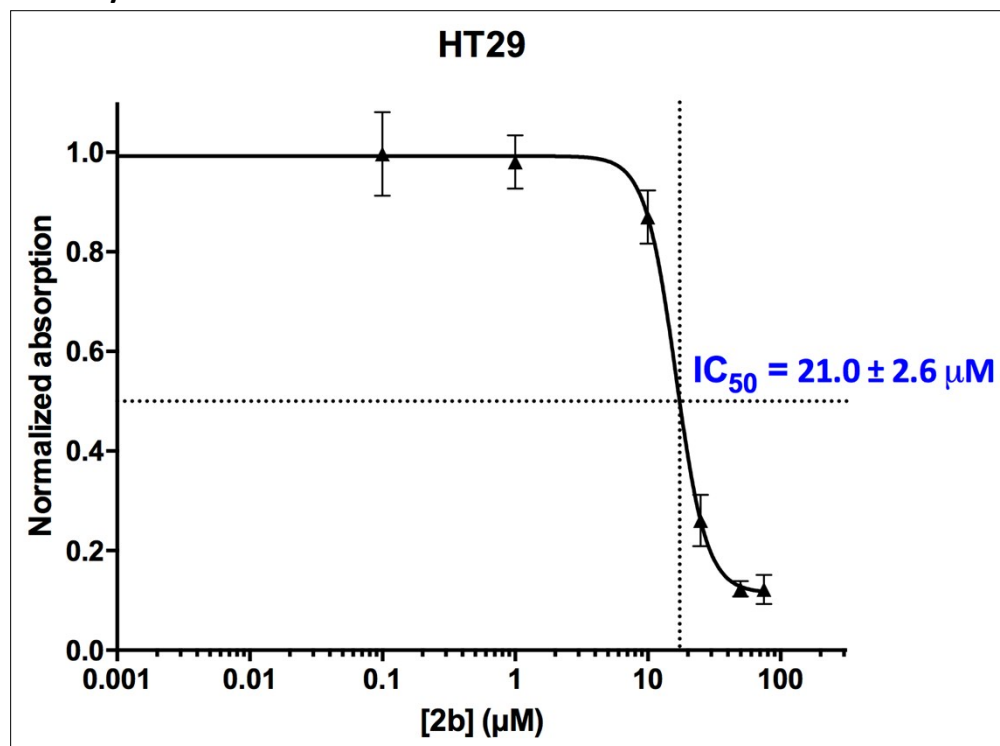


Figure S18. Biological Evaluation of **2b** in HT-29.

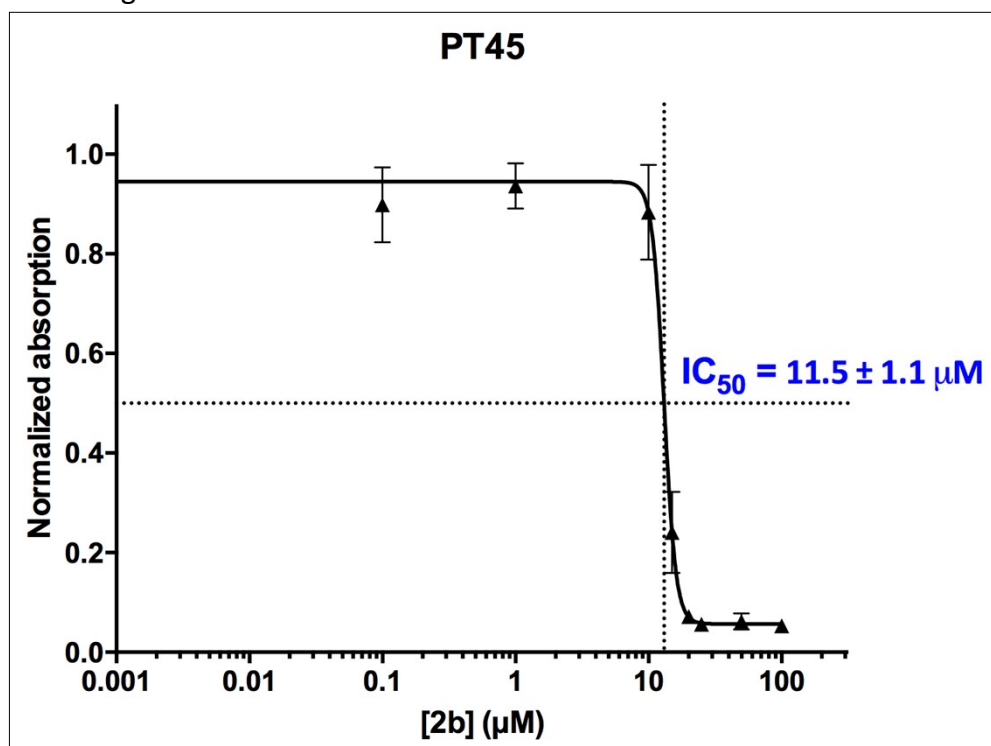


Figure S19. Biological Evaluation of **2b** in PT-45.